High Resolution Airborne Observations of Warm Cloud Microphysics during the initiation of deep convection in the Complex Terrain of Central Argentina during CACTI

Yayun Qiao[1]; Greg McFarquhar[1]; Fan Mei[2]

[1]. University of Oklahoma [2]. Pacific Northwest National Laboratory

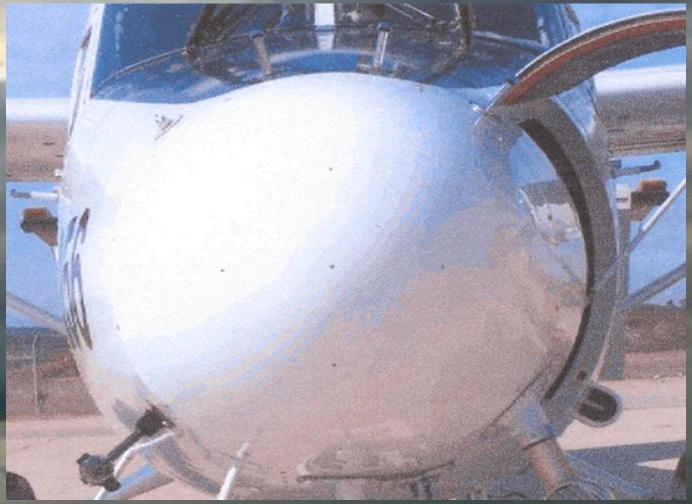

Background - Scientific questions

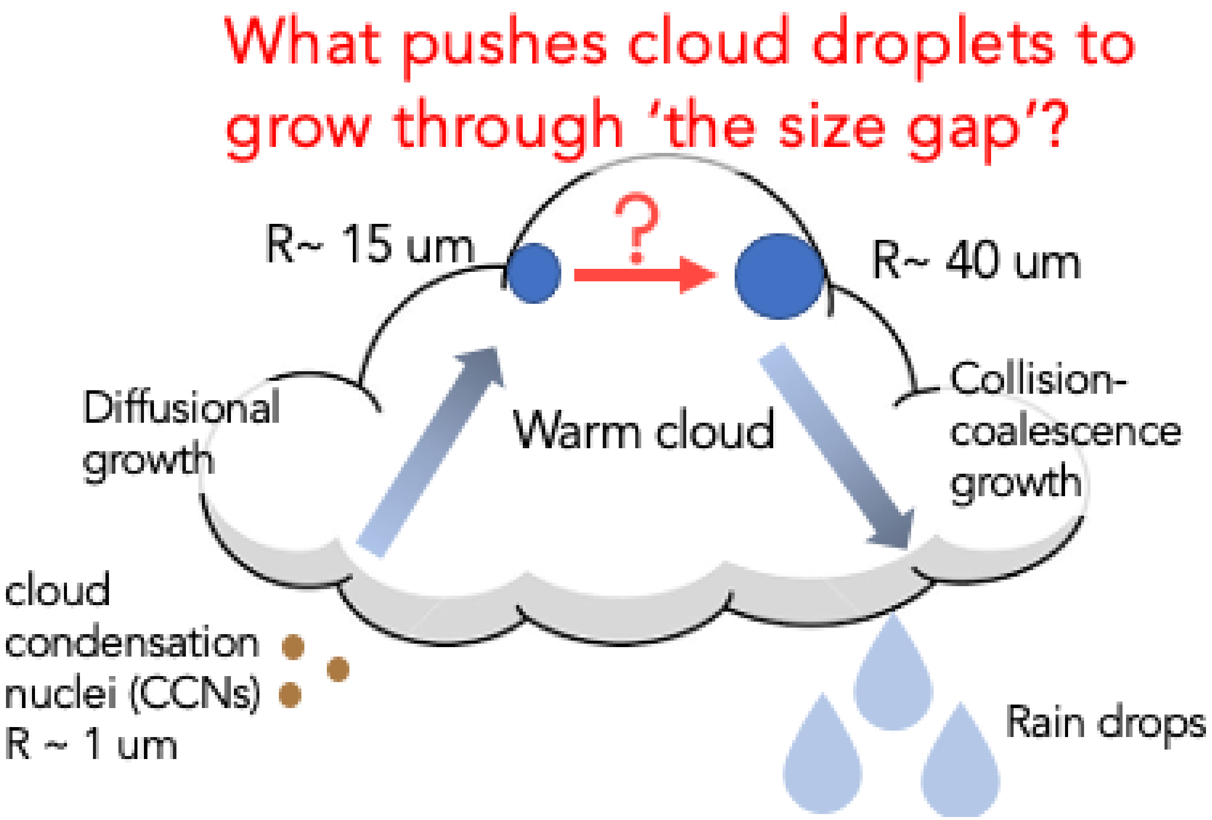

- ❖ Effect of turbulence on entrainment and mixing
- ❖ Effect of turbulence on diffusional growth
- ❖ Effect of turbulence on Collisional growth
- ❖ Effect of grant aerosol particles

Goal: investigate the role of entrainment effects and turbulence play in the "size gap problem ", and further improve model performance.

Observational campaigns - Instrumentations

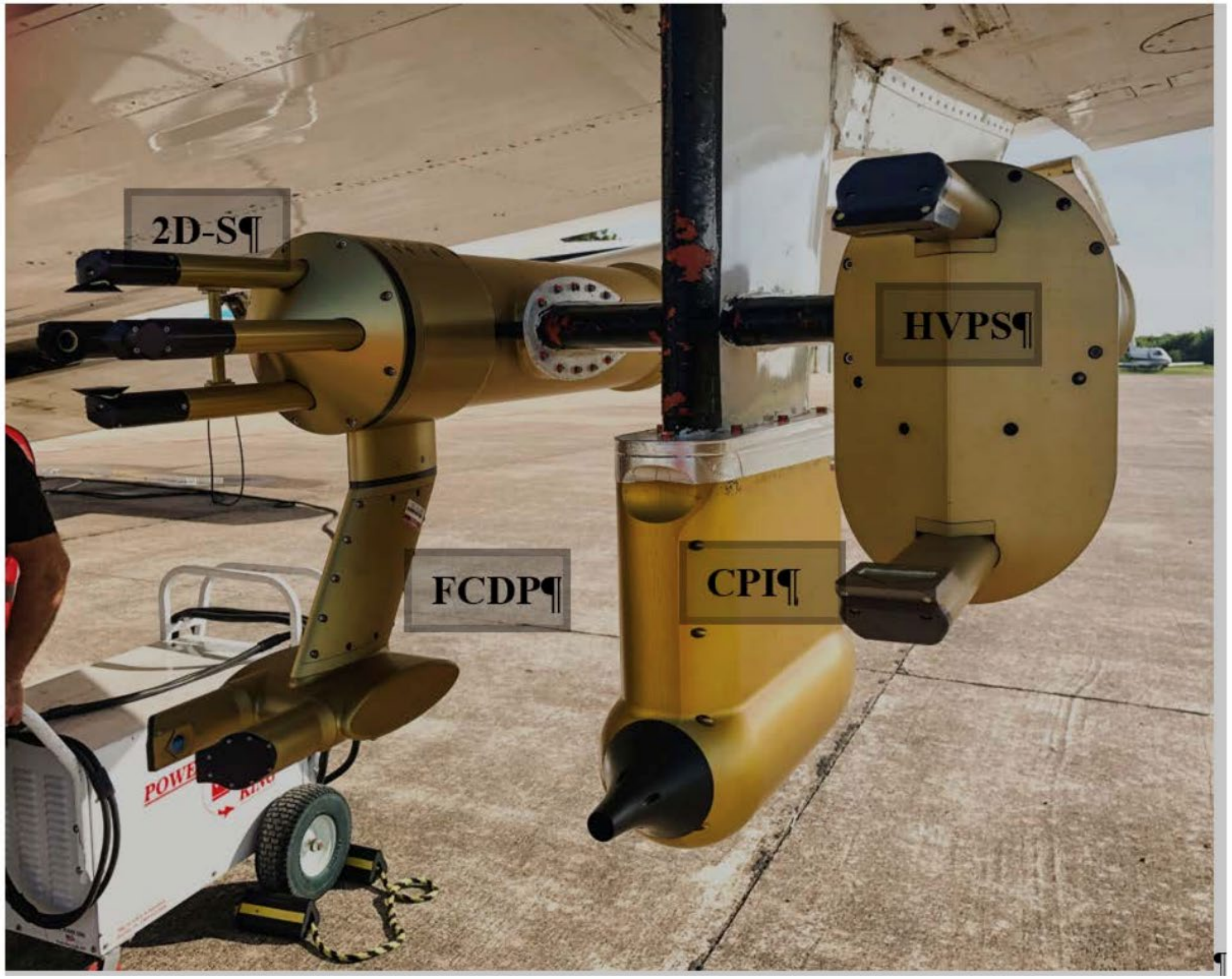

Cloud and aerosol probes deployed under the wings of G1 aircraft

High-resolution dataset

- FCDP (20HZ): number concentration (N), cloud droplet particle size distribution (DSDs), liquid water content (LWC)
- AIMMS-20 (20HZ): temperature (T), relative humidity (R), vertical velocity (W)…

Instrumentation	Ranges
Gust Probe	-
Airborne Integrated Meteorological Measurement System (AIMMS)	-
Passive Cavity Aerosol Spectrometer Probe (PCASP)	0.1 - 3 um
ultra-high-sensitivity aerosol spectrometer (UHSAS)	0.01 - 1 um
CCN Counter	0.75 - 10 um
Fast Cloud Droplet Probe (FCDP)	1 - 50 um
2 Dimensional Stereo Probe (2D-S)	10 - 1280 um

Observational campaigns – CACTI

The Cloud, Aerosol, and Complex Terrain Interactions (CACTI) field campaign

Location: the Sierras de Córdoba range in north-central Argentina

Time: 1 OCTOBER 2018 - 30 APRIL 2019

A total of 7 flight paths from 11/06/2018 and 12/01/2018 with 90 sampled clouds chosen for analysis. The selected cloud paths from 11/06/2018 is indicated by orange shading.

Satellite: GOES 16; Radar: CSAPR2

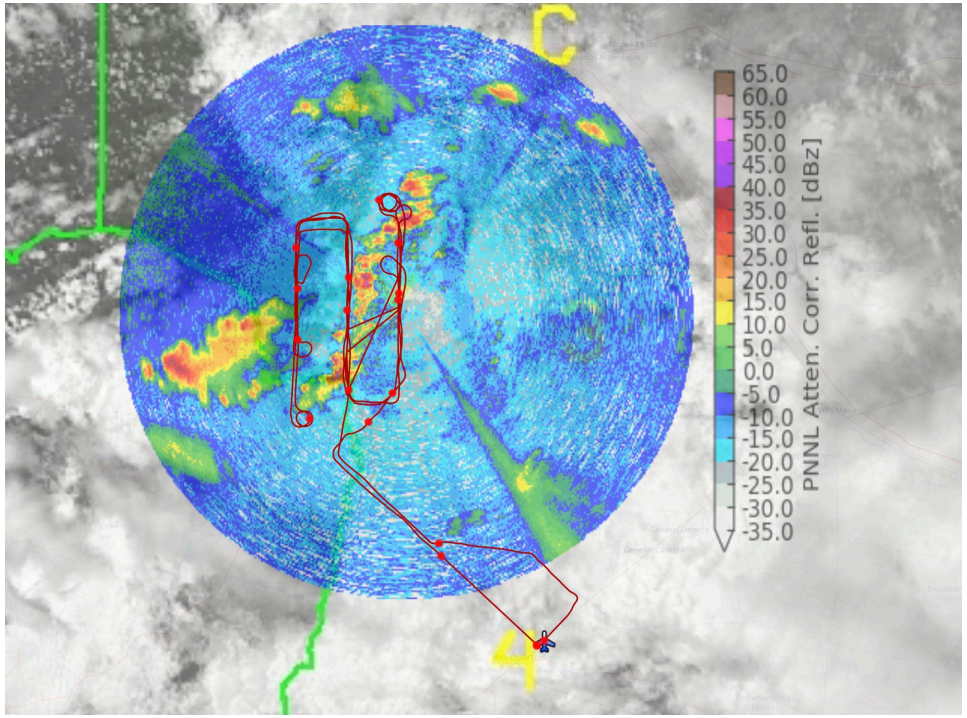

Flight path on 11/06/2018

Selected cloud paths

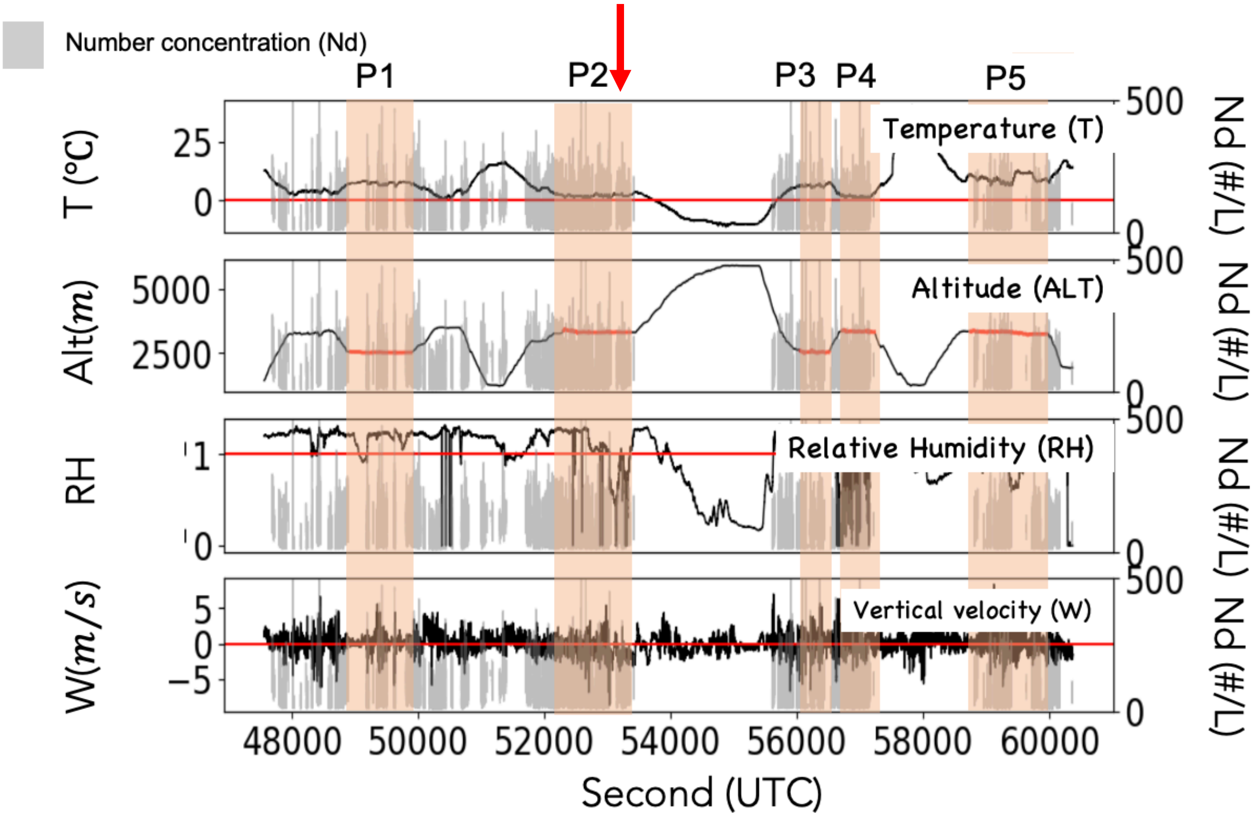

Flight path on 11/06/2018

Results – Adiabatic Fraction (AF)

$$AF = \frac{LWC}{LWC_a}$$

2D histogram between the mean droplet radius ($\bar{R}$), droplet radius dispersion (σ_R), and cloud droplet size distributions (DSDs) relative dispersion $\epsilon = \frac{\sigma_R}{\bar{R}}$ along AF.

- Figure 8.2D histogram between the mean droplet radius ($\bar{R}$), droplet radius dispersion (σ_R), and cloud droplet size distributions (DSDs) relative dispersion ϵ along AF.

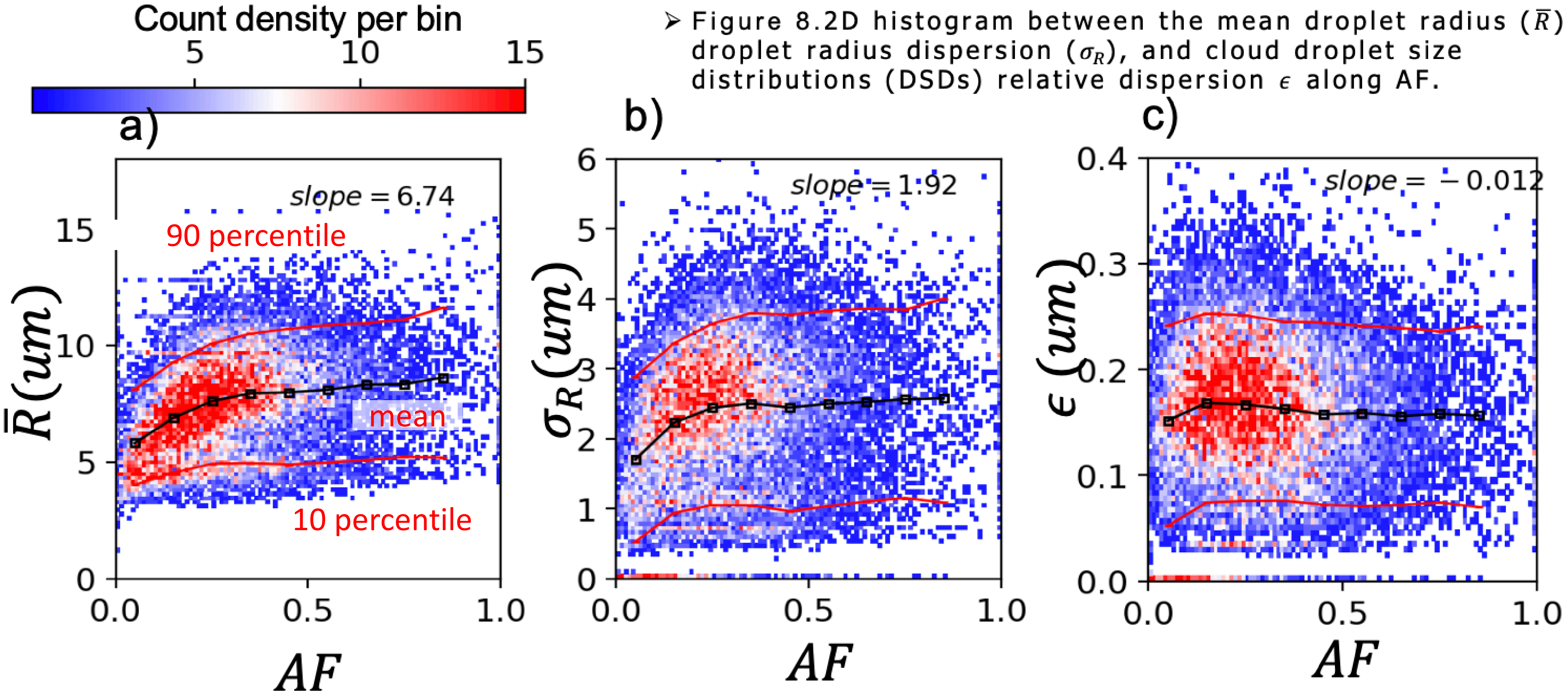

Results – Turbulence

2D histogram between the mean droplet radius ($\bar{R}$), droplet radius dispersion (σ_R), and cloud droplet size distributions (DSDs) relative dispersion $\epsilon = \frac{\sigma_R}{\bar{R}}$ with ${\sigma_w}^2$.

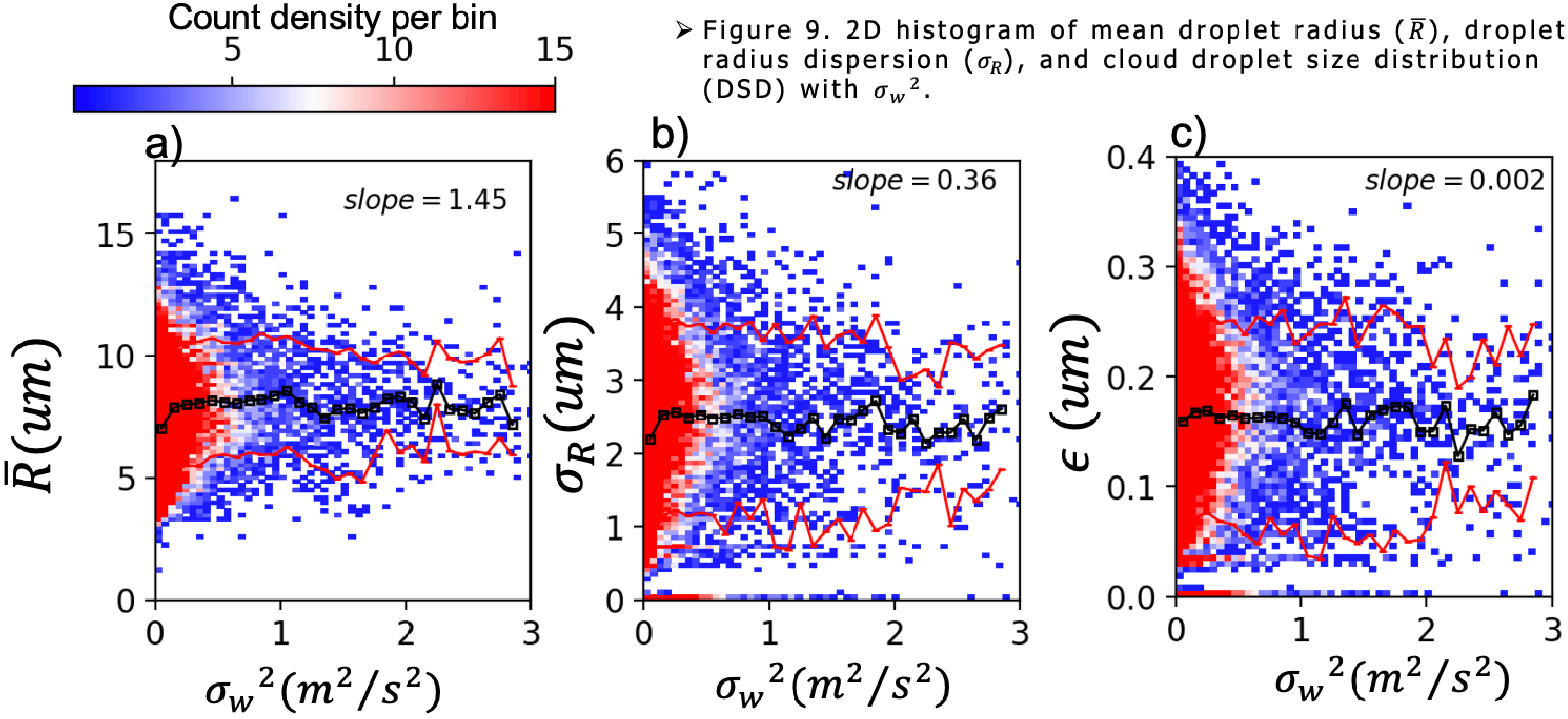

- Figure 9. 2D histogram of mean droplet radius ($\bar{R}$), droplet radius dispersion (σ_R), and cloud droplet size distribution (DSD) with ${\sigma_w}^2$.

Results – Vertical variability

Scatterplot of the AF (left) and ${\sigma_w}^2$ (right) versus the ϵ at three different height above cloud base.

Δz: height above cloud base

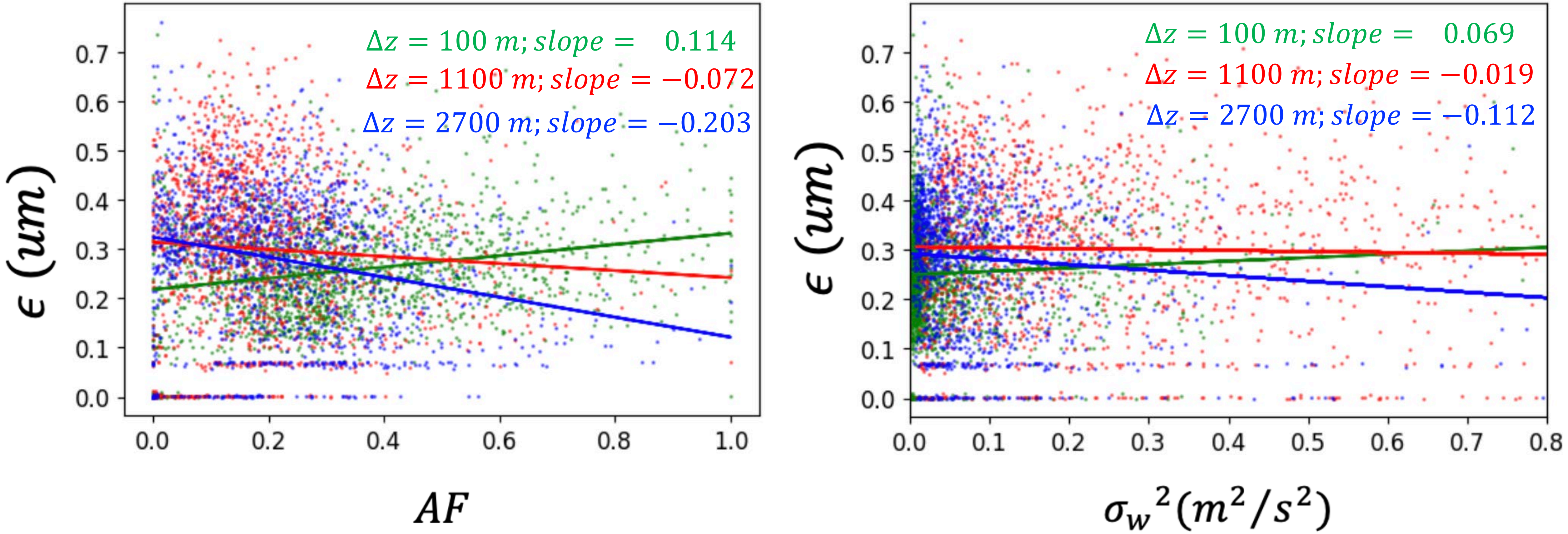

Summery

- 20 HZ High resolution cloud microphysical data used to investigate influence of turbulence and entrainment on particle growth process in warm cloud.

- Weaker evaporation, and stronger condensation in less diluted regions. Particle grow and DSDs broadened when entrainment-mixing is weakened, leading to the decrease of ϵ.

- Two mechanisms associated with ${\sigma_w}^2$ are working against each other on the broadness of DSDs. The relationships between ${\sigma_w}^2$, $\overline{R}$, σ_R, and ϵ may not be prominent because data from all cloud samples analyzed together. To gain more insight, vertical variability of the data will be investigated.

- ϵ has a positive relationship with AF and ${\sigma_w}^2$ near cloud base but these correlation are negative around cloud top.